IEEE Access
Multidisciplinary ⋮ Rapid Review ⋮ Open Access Journal

Received April 10, 2020, accepted April 27, 2020, date of publication May 4, 2020, date of current version May 15, 2020.

Digital Object Identifier 10.1109/ACCESS.2020.2992047

Approximation-Based Adaptive Control of Constrained Uncertain Thermal Management Systems With Nonlinear Coolant Circuit Dynamics of PEMFCs

BYUNG MO KIM AND SUNG JIN YOO
School of Electrical and Electronics Engineering, Chung-Ang University, Seoul 06974, South Korea

Corresponding author: Sung Jin Yoo (sjyoo@cau.ac.kr)

This work was supported in part by the Chung-Ang University Research Scholarship Grants in 2020, and in part by the National Research Foundation of Korea (NRF) Grant funded by the Korea Government under Grant NRF-2019R1A2C1004898.

ABSTRACT This paper addresses an adaptive temperature control problem for preventing the membrane dehydration and electrode flooding of nonlinear proton exchange membrane fuel cells (PEMFCs). Compared with the previous thermal control results of PEMFC temperature systems, the main contributions of this paper are two-fold: (i) nonlinear thermal management systems with nonlinear coolant circuit dynamics are firstly adopted in the temperature control field of PEMFCs and (ii) temperature constraints are considered to avoid the membrane dehydration and electrode flooding phenomena of PEMFCs. It is assumed that all system parameters and nonlinearities of thermal management systems including nonlinear coolant circuit dynamic are unknown. A recursive control design methodology is presented to guarantee the robust regulation and constraint satisfaction of the stack temperature. From the Lyapunov theorem, the stability of the resulting closed-loop system is analyzed.

INDEX TERMS Thermal management systems, nonlinear coolant circuit dynamics, temperature constraints, adaptive control, proton exchange membrane fuel cells (PEMFCs).

I. INTRODUCTION

Proton exchange membrane fuel cells (PEMFCs) have been regarded as one of the most attractive alternative energy sources in the future because of their advantages such as low operating temperature, high energy efficiency, short charging time, and less noise [1], [2]. The PEMFCs are interconnected by multiple subsystems consisting of the hydrogen flow, the humidity, the air supply, and the thermal management systems. Among these subsystems, the control of thermal management system is important for the general operation of PEMFC in the electrochemical reaction. The temperature range for the general operation of the fuel cells is 50–100°C while an optimal temperature is 80°C [3]. Maintaining the optimal temperature against the abrupt change of the external load leads to improve the performance of thermal management systems and to increase the lifetime of fuel cells [4]. Thus, the control problem of thermal management systems has actively appeared. The optimal temperature control problem using the relative humidity was addressed for PEMFCs [5]. In [6], an active disturbance rejection control design was developed for achieving precise temperature regulation of thermal management systems in PEMFCs. In [7], an adaptive thermal control method was presented to control the stack temperature in a certain range. Recently, a fault-tolerant control approach using the sliding mode technique was presented for thermal management systems of PEMFCs with sensor faults [8]. However, these control strategies [5]–[8] were established without the consideration of coolant circuit models that are important for adjusting the stack temperature of PEMFCs.

Basically, PEMFCs provide electricity by an electrochemical exothermic reaction using the oxygen and hydrogen, and the heat generated at this time should be removed by a cooling system [9]. Therefore, the thermal management considering the coolant circuit model is essential for the optimization of stack performance and contributes to the PEMFC technology that is reliable for more practical applications [10]. Despite

The associate editor coordinating the review of this manuscript and approving it for publication was Lei Wang.

this importance, some limited results have been reported for the temperature control in the presence of the coolant circuit model of PEMFCs. A proportional-integral temperature control design based on a thermal circuit was presented in [11]. In [12], a proportional-integral-derivative controller was used to validate the experimental data of water-cooled PEMFCs. A linear-quadratic-regulator-based control scheme for the minimization of the parasitic power of automotive fuel cell cooling systems was introduced in [13]. In [14], a model reference adaptive control problem was investigated to deal with system uncertainties and to control the stack and coolant inlet temperature in PEMFCs. In [15], the modular thermal modelling and model predictive control methods of water-cooled PEMFC systems were presented. However, the existing control strategies [11]–[15] are based on the linearized model of PEMFC systems and thus are only reliable in the neighborhood of the specific operating point. For more practical applications, there have been some attempts to develop thermal controllers for nonlinear PEMFC systems. The fuzzy-based PEMFC temperature and circulating coolant inlet temperature were controlled by adjusting the coolant flux and bypass valve [16]. In [17], a sliding mode control design using an extended Kalman filter was studied to regulate the temperature of PEMFCs. Despite these efforts, the aforementioned results [11]–[17] have two limitations as follows.

(L1) The existing results [11]–[17] did not consider the dynamics of the coolant pump, namely the coolant flux effects were only considered in thermal management Systems. In [16], the coolant pump model reduced to the steady state input-output representation was only considered and the stability of the closed-loop systems was not proved theoretically. Because the coolant flux for controlling the stack temperature can be adjusted by the dynamics of the coolant pump [18], the nonlinear dynamics of the coolant pump should be considered for the temperature control of PEMFCs.

(L2) The previous works [11]–[17] cannot deal with the temperature constraint problem to prevent the membrane dehydration and electrode flooding phenomena. The high stack temperature of the fuel cells may interrupt the transport effects of the reactants and cause the membrane dehydration that deteriorates the cell performance. In addition, the low stack temperature decreases the electrochemical reaction rate and may lead to the water condensation and the electrode flooding that degrade the performance of PEMFC systems [1], [9]. Thus, the total stack temperature should remain within some reasonable ranges to avoid the membrane dehydration and electrode flooding phenomena while controlling the stack temperature of PEMFCs.

Motivated by these limitations, we present an approximation-based temperature control design to deal with the membrane dehydration and electrode flooding problems of uncertain nonlinear PEMFCs. In thermal management systems, a nonlinear coolant circuit dynamics is combined with the nonlinear dynamics of the total stack temperature where temperature constraints are considered. All system parameters and nonlinearities of the thermal management systems are assumed to be unknown. An approximation-based adaptive temperature control scheme is designed by employing the barrier Lyapunov function technique [19] and the dynamic surface design technique [20]. Through the Lyapunov stability analysis, it is shown that temperature constraints are satisfied to avoid the membrane dehydration and electrode flooding and the robust regulation is achieved against unknown system parameters and nonlinearities.

The contributions of this paper are two-fold:

(i) To the best of our knowledge, there are no temperature control studies for dealing with the nonlinear coolant circuit model in the nonlinear thermal model of PEMFCs although the dynamic property of the coolant pump influences the cooling stack highly. Hence, compared with the existing works [5]–[8], [11]–[17], this paper firstly considers the coolant-circuit-based uncertain nonlinear thermal management systems in the temperature control field of PEMFCs where all system parameters and nonlinearities are unknown.

(ii) Compared with the existing control designs [5]–[8], [11]–[17], this paper addresses the membrane dehydration and electrode flooding prevention problem in the temperature control of PEMFCs. Thus, the constraints of the total stack temperature are combined with the thermal control problem of PEMFCs and an adaptive control methodology is developed to ensure the stability of the closed-loop system and the constraint satisfaction of the stack temperature.

The rest of this paper is organized as follows. The stack temperature and coolant circuit models of PEMFCs are introduced in Section II. In Section III, the constrained temperature control problem is formulated for the thermal management systems with the nonlinear coolant circuit dynamics. In Section IV, an approximation-based adaptive control design is presented using the Lyapunov stability analysis. The simulation result of the resulting control system is provided in Section V. Section VI gives the conclusion of this paper.

II. THERMAL CHARACTERISTICS OF PEMFC

A. THERMAL MANAGEMENT MODEL OF NONLINEAR PEMFC

The thermal management model is established using molar conservation principles, the energy balance, and empirical equations [6], [16]. The dynamics of the total stack temperature T_{st} is defined as

$$\frac{dT_{st}}{dt} = \frac{W_{in} - W_{out} + W_{rea} - W_{wc} - W_{amb} - P_{fc}}{m_{st} c_{p.s}} \quad (1)$$

where W_{in} and W_{out} are the input and output of the gas energy flow rate, respectively, W_{rea} is the total power from the electrochemical reaction, W_{wc} denotes the rate of the heat removal, W_{amb} is the rate of heat loss at the stack surface, P_{fc} is the output power of the PEMFC, m_{st} is the mass of the PEMFC stack, and $c_{p.s}$ is the specific heat of the PEMFC. Each variables in (1) are defined as follows.

TABLE 1. System parameters of the thermal management model.

Symbol	Parameter	Value	SI units
A_c	Active area of cell	280	cm^2
F	Faraday constant	96487	$A \cdot s \cdot mol^{-1}$
ΔH	Hydrogen combustion enthalpy	285,500	$J \cdot mol^{-1}$
m_{st}	PEMFC stack mass	17.5	Kg
T_{amb}	Ambient temperature	298.15	K
T_c^{in}	Cathode inlet gases temperature	323.15	K
T_a^{in}	Anode inlet gases temperature	323.15	K
T_{wc}^{in}	Inlet chilling coolant temperature	328.15	K
T_0	Standard temperature	298.15	K
d_m	Membrane thickness	0.0178	cm
P_c	Cathode pressure	2	atm
P_a	Anode pressure	2	atm
R_t	Thermal resistance	0.145	$K \cdot W^{-1}$
$c_{p.H_2}$	Specific heat of hydrogen	28.944	$J \cdot mol^{-1} \cdot K^{-1}$
$c_{p.H_2O}^g$	Specific heat of gaseous water	33.59	$J \cdot mol^{-1} \cdot K^{-1}$
$c_{p.H_2O}^l$	Specific heat of liquid water	78.53	$J \cdot mol^{-1} \cdot K^{-1}$
$c_{p.O_2}$	Specific heat of oxygen	29.696	$J \cdot mol^{-1} \cdot K^{-1}$
$c_{p.N_2}$	Specific heat of nitrogen	29.03	$J \cdot mol^{-1} \cdot K^{-1}$
$c_{p.air}$	Specific heat of air	20.8	$J \cdot mol^{-1} \cdot K^{-1}$
$c_{p.s}$	Specific heat of PEMFC	4000	$J \cdot mol^{-1} \cdot K^{-1}$
J_{com}	Moment of inertia of pump	2.7×10^{-3}	Kg $\cdot m^2$
J_w	Moment of inertia of water	1.2	Kg $\cdot m^2$
C	Physical parameter	0.095	$N \cdot m \cdot A^{-1}$
τ_f	Physical parameter	0.043	$N \cdot m$
λ_{H_2}	Utilization of hydrogen	1.25	-
λ_{O_2}	Utilization of oxygen	2.5	-
n	Number of cells in fuel-cell stack	381	-
k_{cl}	Physical parameter	55.5	-

(i) **Definition of** W_{in}: The input gas energy flow rate W_{in} is obtained as

$$W_{in} = \left(Q_{a.H_2}^{in} c_{p.H_2} + Q_{a.H_2O}^{in} c_{p.H_2O}^g\right)\left(T_a^{in} - T_0\right) + \left(Q_{c.air}^{in} c_{p.air} + Q_{c.H_2O}^{in} c_{p.H_2O}^g\right)\left(T_c^{in} - T_0\right) \quad (2)$$

where $Q_{a.H_2}^{in}$ and $Q_{c.air}^{in}$ denote the hydrogen molar flow rate and the cathode input air molar flow rate, respectively, $Q_{a.H_2O}^{in}$ and $Q_{c.H_2O}^{in}$ are the input vapor molar flow rates of the anode and cathode, respectively, and $c_{p.H_2}$, $c_{p.air}$, $c_{p.H_2O}^g$, T_a^{in}, T_c^{in}, and T_0 are defined in Table 1. Here, $Q_{a.H_2}^{in}$, $Q_{c.air}^{in}$, $Q_{a.H_2O}^{in}$, and $Q_{c.H_2O}^{in}$ are defined as

$$\begin{aligned} Q_{a.H_2}^{in} &= \lambda_{H_2} Q_{a.H_2}^{rea} \\ Q_{c.air}^{in} &= 0.21 \lambda_{O_2} Q_{c.O_2}^{rea} \\ Q_{a.H_2O}^{in} &= \frac{P_{sat}(T_a^{in}) Q_{a.H_2}^{in}}{P_a - P_{sat}(T_a^{in})} \\ Q_{c.H_2O}^{in} &= \frac{P_{sat}(T_c^{in}) Q_{c.air}^{in}}{P_c - P_{sat}(T_c^{in})} \end{aligned} \quad (3)$$

where λ_{H_2}, λ_{O_2}, P_a, and P_c are defined in Table 1, the saturation pressure function $P_{sat}(x)$ is given by [3]

$$\log P_{sat}(x) = -20.92 + 0.143x - (3.39 \times 10^{-4})x^2 + (3.85 \times 10^{-7})x^3 - (1.69 \times 10^{-10})x^4 \quad (4)$$

and $Q_{a.H_2}^{rea}$ and $Q_{c.O_2}^{rea}$ denote the reacted hydrogen molar flow rate and the reacted oxygen molar flow rate, respectively, and are defined as $Q_{a.H_2}^{rea} = 2Q_{c.O_2}^{rea} = nI_{st}/(2F)$ with the number of the cells n, the PEMFC load current I_{st}, and Faraday constant F.

(ii) **Definition of** W_{out}: The output gas energy flow rate W_{out} considering the water generated in the liquid state is represented by

$$W_{out} = \left(Q_{a.H_2}^{out} c_{p.H_2} + Q_{a.H_2O}^{out} c_{p.H_2O}^g + Q_{c.O_2}^{out} c_{p.O_2} + Q_{c.N_2}^{out} c_{p.N_2} + Q_{c.H_2O}^{out} c_{p.H_2O}^g + Q_{c.H_2O}^{gen} c_{p.H_2O}^l\right) \times \left(T_{st} - T_0\right). \quad (5)$$

where $c_{p.H_2}$, $c_{p.H_2O}^g$, $c_{p.O_2}$, $c_{p.N_2}$, and $c_{p.H_2O}^l$ are defined in Table 1, each electrode vapor output molar rates with the

saturated cell inner vapor are defined as

$$\begin{aligned} Q^{out}_{a.H_2} &= Q^{in}_{a.H_2} - Q^{rea}_{a.H_2} \\ Q^{out}_{a.H_2O} &= Q^{in}_{a.H_2O} - \frac{P_{sat}(T_{st})Q^{rea}_{a.H_2}}{P_a - P_{sat}(T_{st})} \\ Q^{out}_{c.O_2} &= Q^{in}_{c.O_2} - Q^{rea}_{c.O_2} \\ Q^{out}_{c.N_2} &= 0.79Q^{in}_{c.air} \\ Q^{out}_{a.H_2O} &= Q^{in}_{c.H_2O} - \frac{P_{sat}(T_{st})Q^{rea}_{c.O_2}}{P_c - P_{sat}(T_{st})} \end{aligned}$$

with $Q^{in}_{c.O_2} = \lambda_{O_2} Q^{rea}_{c.O_2}$, the function P_{sat} defined in (4), and $Q^{gen}_{c.H_2O} = nI_{st}/(2F)$.

(iii) **Definitions of W_{rea}, W_{wc}, and W_{amb}**: The total fuel energy W_{rea} is derived from the electrochemical reaction as follows:

$$W_{rea} = Q^{rea}_{a.H_2} \Delta H \tag{6}$$

where ΔH is the hydrogen combustion enthalpy constant and $Q^{rea}_{a.H_2}$ is the reacted hydrogen molar flow rate defined in (3).

Since the output coolant temperature is the same as the temperature of the stack (i.e, $T^{out}_{wc} = T_{st}$) [6], the rate of heat removal by the coolant W_{wc} is obtained as

$$W_{wc} = k_{cl} W_{cl} c^{l}_{p.H_2O} (T_{st} - T^{in}_{wc}) \tag{7}$$

where k_{cl} is a physical parameter,W_{cl} is the coolant flux, and $c^{l}_{p.H_2O}$ and T^{in}_{wc} are defined in Table 1.

The heat loss rate W_{amb} at the stack surface is expressed as

$$W_{amb} = (T_{st} - T_{amb})/R_t \tag{8}$$

where R_t and T_{amb} are the thermal resistance and ambient temperatures, respectively and their values are defined in Table 1.

(iv) **Definition of P_{fc}**: The output power of entire PEMFC is expressed as

$$P_{fc} = nI_{st} V_c. \tag{9}$$

where n is number of the cells and $I_{st} > 0$ is the load current of the fuel cell. Here, the operating voltage V_c of the fuel cell is defined by combining all voltage drops associated with the activation loss and ohmic loss as follows [21], [22]:

$$V_c = E - V_{act} - V_{ohm}$$

where the open circuit voltage E is defined as

$$\begin{aligned} E &= 1.229 - 8.5 \times 10^{-4}(T_{st} - 298.15) + 4.3085 \times 10^{-5} \\ &\quad \times T_{st}\left(\ln(P_{H_2}) + \frac{1}{2}\ln(P_{O_2}) \right) \\ P_{H_2} &= [P_a/(P_{sat}(T_{st})e^{(1.635i/T^{1.334}_{st})}) - 1]P_{sat}(T_{st}) \\ P_{O_2} &= (P_c - P_{sat}(T_{st}))/(1 + 3.762e^{(0.291i/T^{0.832}_{st})}) \end{aligned}$$

with the current density $i = I_{st}/A_c$ defined by the PEMFC current I_{st} and the active area A_c, the activation overvoltages V_{act} is given by $V_{act} = V_0 + V_a(1 - e^{-10i})$ [22], and the ohmic overvoltages V_{ohm} is defined as $V_{ohm} = iR_{ohm}$. Here, the values of V_0, V_a, and their coefficients can be derived from the empirical process [22] and the ohmic resistance $R_{ohm} = d_m/\sigma_m$ is proportional to the membrane thickness d_m and inversely proportional to the membrane conductivity $\sigma_m = (5.139 \times 10^{-3}\lambda_m - 3.26 \times 10^{-3})e^{(1.155-350/T_{st})}$ with the membrane water content $\lambda_m = 14$ [3].

Using Definitions (i)–(iv), the thermal management system (1) can be represented by

$$\frac{dT_{st}}{dt} = aI_{st} + \phi_1(T_{st}, I_{st}) - \phi_2(T_{st})W_{cl} \tag{10}$$

where a, $\phi_1(T_{st}, I_{st})$, and $\phi_2(T_{st})$ are defined as

$$\begin{aligned} a &= [(Q_1 + Q_2)(T^{in}_c - T_0) + Q_o T_0 + Q_r]/(m_{st} c_{p.s}) \\ \phi_1 &= \Bigg[\frac{3nc^{g}_{p.H_2O}}{4F}\left(\frac{P_{sat}(T_{st})}{P_c - P_{sat}(T_{st})} \right)(T_{st} - T_0)I_{st} \\ &\quad -(Q_o I_{st} + R_t^{-1})T_{st} + T_{amb}R_t^{-1} \\ &\quad -V_c(T_{st}, I_{st})nI_{st} \Bigg]/(m_{st} c_{p.s}) \\ \phi_2 &= k_{cl} c^{l}_{p.H_2O}(T_{st} - T^{in}_{wc})/(m_{st} c_{p.s}) \end{aligned} \tag{11}$$

with

$$\begin{aligned} Q_1 &= \lambda_H c_{p.H_2} + \lambda_O c_{p.air}, \\ Q_2 &= c^{g}_{p.H_2O}\lambda_{HO}\frac{P_{sat}(T^{in}_c)}{P_c - P_{sat}(T^{in}_c)},\ Q_r = \frac{n\Delta H}{2F}, \\ \lambda_H &= \frac{n\lambda_{H_2}}{2F},\ \lambda_O = \frac{n\lambda_{O_2}}{4 \cdot 0.21F},\ \lambda_{HO} = \lambda_H + \lambda_O \\ Q_o &= \frac{n}{4F}\Bigg(2(\lambda_{H_2} - 1)c_{p.H_2} + (\lambda_{O_2} - 1)c_{p.O_2} \\ &\quad +3.76\lambda_{O_2} c_{p.N_2} + 2c^{l}_{p.H_2O} \\ &\quad +c^{g}_{p.H_2O}\frac{P_{sat}(T^{in}_c)}{P_c - P_{sat}(T^{in}_c)}(2\lambda_{H_2} + \lambda_{O_2}/0.21) \Bigg) \\ V_c(T_{st}, I_{st}) &= 0.95 + (1.2545 \times 10^{-5})T_{st} \\ &\quad -v_{a1}(1.79P_c - 0.79P_{sat}(T_{st}))^2 \\ &\quad -v_{a2}(1.79P_c - 0.79P_{sat}(T_{st})) \\ &\quad -v_{a3} - \frac{d_m I_{st} e^{(-1.155+350/T_{st})}}{A_c(0.005139\lambda_m - 0.00326)} \\ v_{a1}(T_{st}) &= (1.618 \times 10^{-2})(1 - 10^{-3}T_{st}), \\ v_{a2}(T_{st}) &= (1.8 \times 10^{-4})T_{st} - 0.166, \\ v_{a3}(T_{st}) &= (-5.8 \times 10^{-4})T_{st} + 0.5736 \end{aligned}$$

and their physical parameters are given in Table 1.

B. NONLINEAR COOLANT CIRCUIT DYNAMICS WITH FLUX AND PUMP MODELS

In [18], the dynamic model of the coolant circuit with the 36V motor centrifugal pump was derived based on the fundamental relationships among the motor-armature current, motor speed and coolant flow rate. In this model, the coolant flux can be manipulated using a variable speed pump without a control valve. Thus, the weight and complexity of the system can be reduced [18]. The dynamics of the coolant

TABLE 2. Parameters of the coolant system [18].

Parameters	values	Parameters	values
c_1	8.295961	c_4	0.9638
c_2	0.060204	c_5	35.681
c_3	0.0001167	c_6	0.2372
		c_7	0.006531

management system is given by

$$\begin{aligned}\frac{dW_{cl}}{dt} &= c_1 W_{cl}^2 - c_2 W_{cl}\omega_r + c_3\omega_r^2 - \frac{1}{J_w}\\ \frac{d\omega_r}{dt} &= c_4\omega_r + c_5 W_{cl}^2 + c_6 W_{cl}\omega_r - c_7\omega_r^2\\ &\quad -\frac{\tau_f}{J_{com}} + \frac{C}{J_{com}} I_m \end{aligned} \tag{12}$$

where W_{cl} is the coolant flux, ω_r is the angular velocity of the coolant pump motor, I_m is the input motor-armature current of the coolant pump, the constants J_w, J_{com}, τ_f, and C are given in Table 1, and the coefficients $c_1, \ldots, c_7$ are given in Table 2.

III. PROBLEM FORMULATION

A. THERMAL MANAGEMENT SYSTEMS WITH NONLINEAR COOLANT CIRCUIT DYNAMICS

Let us define the variables $x_1 = T_{st}$, $x_2 = W_{cl}$, $x_3 = \omega_r$, $\delta = I_{st}$, and $u = I_m$. Then, the thermal management system with a 75-kW fuel cell stack and a 36V motor centrifugal coolant pump (i.e., (10) and (12)) can be rewritten by the following state-space model

$$\begin{aligned}\dot{x}_1 &= a\delta + \phi_1(x_1, \delta) - \phi_2(x_1)x_2\\ \dot{x}_2 &= \phi_3(x_2, x_3)\\ \dot{x}_3 &= \phi_4(x_2, x_3) + bu\\ y &= x_1 \end{aligned} \tag{13}$$

where $\phi_3 = c_1 x_2^2 - c_2 W_{cl}\omega_r + c_3\omega_r^2 - 1/J_w$, and $\phi_4 = c_4 x_3 + c_5 x_2^2 + c_6 x_2 x_3 - c_7 x_3^2 - \tau_f/J_{com}$ and $b = C/J_{com}$.

Assumption 1: The system parameters a, b and the functions ϕ_1, ϕ_2, ϕ_3, and ϕ_4 are unknown.

Lemma 1 [23]: The inequality $|\mu| \le \mu\tanh(\mu/\kappa) + 0.2785\kappa$ is ensured for any constant $\kappa > 0$ and $\mu \in \mathbb{R}$.

Lemma 2 [24]: For the interval $-k_c < z < k_c$ with any $z \in \mathbb{R}$ and $k_c \in \mathbb{R}$, it holds that

$$\log\left(\frac{k_c^2}{k_c^2 - z^2}\right) \le \frac{z^2}{k_c^2 - z^2}.$$

B. CONSTRAINED TEMPERATURE CONTROL PROBLEM

The temperature management has been recognized as one of significant technical challenges of PEMFCs. The high cell temperature causes membrane dehydration because of the insufficient water supply to PEMFC and the low cell temperature may lead to electrode flooding caused by water condensation, consequently to hinder reactant mass transport with a resultant voltage loss [1], [9]. Based on [3], the optimal value of the total stack temperature is $y_r = 353K$. Thus, it is important to consider the regulation problem of thermal management control systems with temperature constraints. To this end, the constraints of the total stack temperature y are considered as

$$y_r - k_c \le y \le y_r + k_c, \quad \forall t \ge 0. \tag{14}$$

where the constant k_c denotes the physical temperature constraint to prevent the membrane dehydration and the electrode flooding of PEMFCs. If the initial stack temperature $y(0)$ does not remain within the constraints, it means that PEMFCs are under the membrane dehydration and electrode flooding phenomena at the initial time. This is not reasonable for the stable operation of PEMFCs. Thus, it is assumed that the initial stack temperature $y(0)$ satisfies the constraints (14).

Property 1: For system (13), there exists an unknown positive constant $\underline{\phi}_2$ such that $0 < \underline{\phi}_2 \le \phi_2$.

Proof: The function $\phi_2(x_1)$ is defined as $\phi_2(x_1) = k_{cl} c_{p.H_2O}^l (x_1 - T_{wc}^{in})/(m_{st} c_{p.s})$. In Table 1, it holds that $m_{st} c_{p.s} > 0$, $c_{p.H_2O}^l > 0$, $k_{cl} > 0$, and $T_{wc}^{in} > 0$. Additionally, since the output coolant temperature is the same as the temperature of the stack and is larger than the inlet chilling coolant temperature T_{wc}^{in} [3], $x_1 > T_{wc}^{in}$ is ensured. Therefore, Property 1 is satisfied. ■

Problem 1: Consider the uncertain thermal management system (13) with temperature constraints (14) of the PEMFC. The main control problem is to find approximation-based adaptive control law u so that the system output y follows the optimal value y_r within the constraints (14).

Remark 1: Contrary to the previous temperature control methods for thermal management systems of PEMFCs [5]–[8], [11]–[17], the nonlinear coolant circuit dynamics (12) with flux and pump models is firstly considered with the nonlinear stack temperature dynamics (10) for the temperature control problem of PEMFCs. Furthermore, the temperature constraint problem is addressed to prevent the membrane dehydration and electrode flooding of PEMFCs. Therefore, a solution on Problem 1 cannot be suggested in the previous works [5]–[8], [11]–[17].

IV. ADAPTIVE TEMPERATURE CONTROL IN THE PRESENCE OF NONLINEAR COOLANT CIRCUIT DYNAMICS

A. RADIAL BASIS FUNCTION NEURAL NETWORKS

For the online approximation of unknown nonlinear functions W_i, $i = 1, 2, 3$, to be defined in the controller design, radial basis function neural networks (RBFNNs) are used. Using the universal approximation property of the RBFNN [25], [26], for continuous real-valued function $W_i(\varrho_i) : D_{\varrho_i} \mapsto \mathbb{R}$ with a compact set $D_{\varrho_i} \subset \mathbb{R}^{q_i}$, there exists the ideal weight vector θ_i^* with a sufficiently large q_i such that

$$W_i(\varrho_i) = \theta_i^{*\top}\xi_i(\varrho_i) + \psi_i(\varrho_i) \tag{15}$$

where $i = 1, 2, 3$, $\varrho_i = [\varrho_{i,1}, \ldots, \varrho_{i,q_i}]^\top \in D_{\varrho_i}$ and ψ_i are the input vector and the network reconstruction error,

respectively, $\theta_i^* \in \mathbb{R}^{r_i}$ is the optimal weighting vector defined as $\theta_i^* = \text{argmin}_{\hat{\theta}_i}[\sup_{\varrho_i \in D_{\varrho_i}} |W_i(\varrho_i) - \hat{\theta}_i^\top \xi_i(\varrho_i)|]$ with the node number $r_i > 1$ and the estimate $\hat{\theta}_i$ of θ_i^*, and $\xi_i(\varrho_i) = [\xi_{i,1}(\varrho_i), \xi_{i,2}(\varrho_i), \ldots, \xi_{i,r_i}(\varrho_i)]^\top \in \mathbb{R}^{r_i}$; $\xi_{i,j}(\varrho_i) = e^{-\|\varrho_i - c_{i,j}\|^2/\iota_{i,j}^2}$, $j = 1, \ldots, r_i$ denotes the Gaussian function with the center of the receptive field $c_{i,j} = [c_{i,j,1}, \ldots, c_{i,j,q_i}]^\top \in \mathbb{R}^{q_i}$ and the width $\iota_{i,j} \in \mathbb{R}$.

Assumption 2 [25]: The optimal weighting vector and reconstruction error are bounded as $\|\theta_i^*\| \le \bar{\theta}_i$ and $|\psi_i| \le \psi_i^*$ with unknown constants $\bar{\theta}_i > 0$ and $\psi_i^* > 0$, respectively.

B. DESIGN OF ADAPTIVE CONTROLLER

In this section, an approximation-based adaptive controller design strategy is presented for system (13) with the output constraint (14). For the dynamic surface design [20], the error surfaces and the boundary layer errors are defined as

$$\begin{aligned} z_1 &= y - y_r \\ z_2 &= x_2 - \alpha_{1f} \\ z_3 &= x_3 - \alpha_{2f} \\ \epsilon_1 &= \alpha_{1f} - \alpha_1 \\ \epsilon_2 &= \alpha_{2f} - \alpha_2 \end{aligned} \tag{16}$$

where z_1, z_2 and z_3 are control error surfaces, ϵ_1 and ϵ_2 are boundary layer errors, α_1 and α_2 are the virtual control laws, and α_{1f} and α_{2f} are the signals derived from the first-order filters with the time constants $\nu_1, \nu_2 > 0$ as follows:

$$\begin{aligned} \nu_1 \dot{\alpha}_{1f} + \alpha_{1f} &= \alpha_1, \quad \alpha_{1f}(0) = \alpha_1(0) \\ \nu_2 \dot{\alpha}_{2f} + \alpha_{2f} &= \alpha_2, \quad \alpha_{2f}(0) = \alpha_2(0). \end{aligned} \tag{17}$$

The recursive control design consists of three steps. In the first step, the adaptive virtual control law α_1 is designed to stabilize the dynamics of the first error surface z_1 for the regulation of the stack temperature x_1 while the stack temperature constraints (14) are satisfied. To this end, the Lyapunov stability analysis strategy using a barrier function is established. In the second step, the adaptive virtual control law α_2 is designed to stabilize the dynamics of the second error surface z_2 based on the flux dynamics of the nonlinear coolant circuit (12). In the third step, the adaptive actual control law u denoting the input motor-armature current of the coolant pump is designed to stabilize the dynamics of the third error surface z_3. For the stable control design, the Lyapunov stability theorem [27] is used in these design steps. In addition, the first-order low-pass filters (17) based on the dynamic surface design technique are employed to avoid the calculation of the time derivative of the virtual control laws in the recursive design.

Step 1: The time derivative of z_1 along the first equation of (13) is given by

$$\dot{z}_1 = a\delta + \phi_1(x_1, \delta) - \phi_2(x_1)x_2. \tag{18}$$

The output constraint problem (14) can be redefined as the constraint problem of z_1 as follows:

$$-k_c < z_1(t) < k_c. \tag{19}$$

From (19), we consider the following barrier Lyapunov function

$$V_{z_1} = \frac{1}{2} \log \frac{k_c^2}{k_c^2 - z_1^2} \tag{20}$$

where log denotes the natural logarithm.

Differentiating V_{z_1} with respect to time yields

$$\dot{V}_{z_1} = \frac{z_1 \dot{z}_1}{(k_c^2 - z_1^2)} = \rho_c \dot{z}_1 \tag{21}$$

where $\rho_c = z_1/(k_c^2 - z_1^2)$. Then, $\dot{V}_{z_1}$ along (16) and (18) becomes

$$\dot{V}_{z_1} = \rho_c(a\delta + \phi_1(x_1, \delta) - \phi_2(x_1)(z_2 + \epsilon_1 + \alpha_1)). \tag{22}$$

From Lemma 1, it holds that

$$\begin{aligned} \rho_c a\delta &\le |\rho_c| a\delta \\ &\le \rho_c \tanh\left(\frac{\rho_c}{\kappa_0}\right) a\delta + 0.2785 a\delta\kappa_0 \\ &\le \rho_c \tanh\left(\frac{\rho_c}{\kappa_0}\right) a\delta \frac{\phi_2}{\underline{\phi}_2} + 0.2785 a\delta\kappa_0 \frac{\phi_2}{\underline{\phi}_2} \end{aligned} \tag{23}$$

where $\kappa_0 > 0$ is a constant.

Then $\dot{V}_{z_1}$ becomes

$$\begin{aligned} \dot{V}_{z_1} \le \rho_c \phi_2 \Bigg(&- z_2 - \epsilon_1 - \alpha_1 + \frac{\phi_1}{\phi_2} + \tanh\left(\frac{\rho_c}{\kappa_0}\right) \bar{a}\delta \Bigg) \\ &+ 0.2785 \bar{a}\delta\kappa_0\phi_2 \end{aligned} \tag{24}$$

where $\bar{a} = a/\underline{\phi}_2$.

Now, the Lyapunov function V_1 is considered as

$$V_1 = \frac{1}{\phi_2} V_{z_1} + \frac{1}{2}\left(\tilde{\theta}_1^\top \gamma_1^{-1} \tilde{\theta}_1 + \gamma_2^{-1} \tilde{\psi}_1^2 + \gamma_3^{-1} \tilde{a}^2\right)$$

where $\tilde{\theta}_1 = \theta_1^* - \hat{\theta}_1$, $\tilde{\psi}_1 = \psi_1^* - \hat{\psi}_1$, $\tilde{a} = \bar{a} - \hat{a}$; $\hat{\theta}_1$, $\hat{\psi}_1$, and $\hat{a}$ are estimates of θ_1^*, ψ_1^*, and $\bar{a}$, respectively, $\gamma_1 > 0$ is a tuning matrix, and $\gamma_2 > 0$ and $\gamma_3 > 0$ are tuning constants.

The time derivative of V_1 along (24) and (23) becomes

$$\begin{aligned} \dot{V}_1 = \rho_c \Bigg(&- z_2 - \epsilon_1 - \alpha_1 + W_1(\varrho_1) + \tanh\left(\frac{\rho_c}{\kappa_0}\right) \bar{a}\delta \Bigg) \\ &- \tilde{\theta}_1^\top \gamma_1^{-1} \dot{\hat{\theta}}_1 - \gamma_2^{-1} \tilde{\psi}_1 \dot{\hat{\psi}}_1 - \gamma_3^{-1} \tilde{a}\dot{\hat{a}} + 0.2785 \bar{a}\delta\kappa_0 \end{aligned} \tag{25}$$

where $W_1(\varrho_1) = \phi_1/\phi_2 - (\dot{\phi}_2/\rho_c\phi_2^2)V_{z_1}$; $\varrho_1 = x_1$. Based on (15) and Assumption 2, the unknown nonlinearity W_1 is estimated by $W_1(\varrho_1) = \theta_1^{*\top} \xi_1 + \psi_1$.

From Lemma 1, it holds that

$$\begin{aligned} \rho_c \psi_1 &\le |\rho_c| \psi_1^* \\ &\le \rho_c \tanh\left(\frac{\rho_c}{\kappa_1}\right) \psi_1^* + 0.2785 \kappa_1 \psi_1^* \end{aligned} \tag{26}$$

where $\kappa_1 > 0$ is a constant. Then, (25) becomes

$$\dot{V}_1 \le \rho_c\Big(- z_2 - \epsilon_1 - \alpha_1 + \tanh\left(\frac{\rho_c}{\kappa_0}\right)\bar{a}\delta + \theta_1^{*\top}\xi_1 + \tanh\left(\frac{\rho_c}{\kappa_1}\right)\psi_1^*\Big) - \tilde{\theta}_1^\top\gamma_1^{-1}\dot{\hat{\theta}}_1 - \gamma_2^{-1}\tilde{\psi}_1\dot{\hat{\psi}}_1 - \gamma_3^{-1}\tilde{a}\dot{\hat{a}} + C_1 \quad (27)$$

where $C_1 = 0.2785\bar{a}\delta\kappa_0 + 0.2785\kappa_1\psi_1^*$.

The first adaptive virtual control law α_1 with adaptation laws for $\hat{\theta}_1$, $\hat{\psi}_1$, and $\hat{a}$ is presented as

$$\alpha_1 = \zeta_1 z_1 + \frac{1}{2}\rho_c + \hat{\theta}_1^\top\xi_1 + \tanh\left(\frac{\rho_c}{\kappa_1}\right)\hat{\psi}_1 + \tanh\left(\frac{\rho_c}{\kappa_0}\right)\hat{a}\delta \quad (28)$$

$$\dot{\hat{\theta}}_1 = \gamma_1(\rho_c\xi_1 - \sigma_1\hat{\theta}_1) \quad (29)$$

$$\dot{\hat{\psi}}_1 = \gamma_2\left(\rho_c\tanh\left(\frac{\rho_c}{\kappa_1}\right) - \sigma_2\hat{\psi}_1\right) \quad (30)$$

$$\dot{\hat{a}} = \gamma_3\left(\rho_c\tanh\left(\frac{\rho_c}{\kappa_0}\right)\delta - \sigma_3\hat{a}\right) \quad (31)$$

where $\zeta_1 > 0$ denotes a design parameter and $\sigma_1 > 0, \sigma_2 > 0$, $\sigma_3 > 0$ are the design parameters for σ-modification [28].

Substituting (28)–(31) into (27) yields

$$\dot{V}_1 \le -\zeta_1\rho_c z_1 - \frac{1}{2}\rho_c^2 - \rho_c(z_2 + \epsilon_1) + \sigma_1\tilde{\theta}_1^\top\hat{\theta}_1 + \sigma_2\tilde{\psi}_1\hat{\psi}_1 + \sigma_3\tilde{a}\hat{a} + C_1. \quad (32)$$

Following the inequality $|\rho_c\epsilon_1| \le (1/2)\rho_c^2 + (1/2)\epsilon_1^2$, we have

$$\dot{V}_1 \le -\zeta_1\rho_c z_1 - \rho_c z_2 + \frac{1}{2}\epsilon_1^2 + \sigma_1\tilde{\theta}_1^\top\hat{\theta}_1 + \sigma_2\tilde{\psi}_1\hat{\psi}_1 + \sigma_3\tilde{a}\hat{a} + C_1. \quad (33)$$

Remark 2: The adaptive virtual control law (28) with the adaptive laws (29)–(31) is designed in the first step where the barrier Lyapunov function (20) is employed to deal with the stack temperature constraint problem. From the Lyapunov stability analysis, the adaptive laws (29) and (30) are derived to tune the weighting vector of the neural-network-based function approximator $\hat{\theta}_1^\top\xi_1$ and to compensate for the unknown reconstruction error ψ_1, respectively. In addition, the adaptive law (31) is derived to compensate for the unknown parameter $\bar{a}$.

Step 2: Consider $\dot{x}_2 = \phi_3(x_2, x_3)$. The time derivative of z_2 is $\dot{z}_2 = \phi_3(x_2, x_3) - \dot{\alpha}_{1f}$. Using the mean value theorem [29], the function ϕ_3 is represented by

$$\phi_3(x_2, x_3) = \phi_3(x_2, \alpha^*) + h_\vartheta(x_3 - \alpha^*) \quad (34)$$

where $h_\vartheta(\bar{x}_\vartheta) = \partial\phi_3(x_2, x_3)/\partial x_3|_{x_3 = x_\vartheta}$ with $x_\vartheta = \vartheta x_3 + (1-\vartheta)\alpha^*$; $\bar{x}_\vartheta = [x_2, x_\vartheta]^\top$, $0 < \vartheta < 1$ and $\alpha^*(x_2)$ is a smooth function.

Property 2: The sign of the unknown function h_ϑ is positive, and it is satisfied that $0 < h_{\vartheta_0} \le h_\vartheta$ where h_{ϑ_0} is an unknown constant.

Proof: From the definition of ϕ_3, we have $\partial\phi_3/(\partial x_3) = -c_2x_2 + 2c_3x_3$. Based on the prediction data given in Table 2 of [18], it is ensured that $\partial\phi_3/\partial x_3 > 0$ in the practical operation range of the coolant circuit dynamics (12). Additionally, $0 < h_{\vartheta_0} \le h_\vartheta$ is ensured with an unknown constant h_{ϑ_0}. ■

Assumption 3: There exists an unknown constant $h_{\vartheta_d} > 0$ such that $|\dot{h}_\vartheta(\cdot)| \le h_{\vartheta_d}$ for all $\bar{x}_\vartheta \in \Omega_x \subset \mathbb{R}^2$ with the compact region Ω_x.

Using the implicit function theorem [27], $\alpha^*(x_2)$ satisfies $\phi_3(x_2, \alpha^*) = 0$. Thus, $\dot{z}_2$ becomes

$$\dot{z}_2 = h_\vartheta(z_3 + \epsilon_2 + \alpha_2 - \alpha^*) - \dot{\alpha}_{1f}. \quad (35)$$

Consider the following Lyapunov function V_2

$$V_2 = \frac{1}{2h_\vartheta}z_2^2 + \frac{1}{2}\left(\tilde{\theta}_2^\top\gamma_4^{-1}\tilde{\theta}_2 + \gamma_5^{-1}\tilde{\psi}_2^2\right) \quad (36)$$

where $\gamma_4 > 0$ is a tuning matrix, $\gamma_5 > 0$ is a tuning gain, and $\tilde{\theta}_2 = \theta_2^* - \hat{\theta}_2$ and $\tilde{\psi}_2 = \psi_2^* - \hat{\psi}_2$; $\hat{\theta}_2$ and $\hat{\psi}_2$ are estimates of θ_2^* and ψ_2^*, respectively.

The time derivative of V_2 is obtained as

$$\dot{V}_2 = z_2(z_3 + \epsilon_2 + \alpha_2 + W_2(\varrho_2)) - \tilde{\theta}_2^\top\gamma_4^{-1}\dot{\hat{\theta}}_2 - \gamma_5^{-1}\tilde{\psi}_2\dot{\hat{\psi}}_2 \quad (37)$$

where $W_2(\varrho_2) = -\alpha^* - (\alpha_1 - \alpha_{1f})/(\nu_1 h_\vartheta) + (h_{\vartheta_d}/2h_{\vartheta_0}^2)z_2$; $\varrho_2 = [x_2, (\alpha_1 - \alpha_{1f})/\nu_1, z_2]^\top$ owing to $\dot{\alpha}_{1f} = (\alpha_1 - \alpha_{1f})/\nu_1$. From (15) and Assumption 2, the nonlinear function W_2 is approximated by $W_2(\varrho_2) = \theta_2^{*\top}\xi_2 + \psi_2$.

Then, using the inequality

$$z_2\psi_2 \le |z_2|\psi_2^* \le z_2\tanh\left(\frac{z_2}{\kappa_2}\right)\psi_2^* + 0.2785\kappa_2\psi_2^* \quad (38)$$

with a constant $\kappa_2 > 0$, (37) becomes

$$\dot{V}_2 = z_2\left(z_3 + \epsilon_2 + \alpha_2 + \theta_2^{*\top}\xi_2 + \tanh\left(\frac{z_2}{\kappa_2}\right)\psi_2^*\right) - \tilde{\theta}_2^\top\gamma_4^{-1}\dot{\hat{\theta}}_2 - \gamma_5^{-1}\tilde{\psi}_2\dot{\hat{\psi}}_2 + C_2 \quad (39)$$

where $C_2 = 0.2785\kappa_2\psi_2^*$.

The virtual control law α_2 with the adaptation parameters $\hat{\theta}_2$ and $\hat{\psi}_2$ is chosen as

$$\alpha_2 = -\zeta_2 z_2 + \rho_c - \hat{\theta}_2^\top\xi_2 - \tanh\left(\frac{z_2}{\kappa_2}\right)\hat{\psi}_2 - \frac{1}{2}z_2 \quad (40)$$

$$\dot{\hat{\theta}}_2 = \gamma_4(z_2\xi_2 - \sigma_4\hat{\theta}_2) \quad (41)$$

$$\dot{\hat{\psi}}_2 = \gamma_5\left(z_2\tanh\left(\frac{z_2}{\kappa_2}\right) - \sigma_5\hat{\psi}_2\right) \quad (42)$$

where $\zeta_2 > 0$ is a control gain and $\sigma_4 > 0$ and $\sigma_5 > 0$ are the design parameters for the σ-modification [28].

Using (40)–(42), Property 1, and Assumption 2, (39) becomes

$$\dot{V}_2 \le -\zeta_2 z_2^2 + \rho_c z_2 - \frac{1}{2}z_2^2 + z_2(z_3 + \epsilon_2) + \sigma_4\tilde{\theta}_2^\top\hat{\theta}_2 + \sigma_5\tilde{\psi}_2\hat{\psi}_2 + C_2. \quad (43)$$

Using the inequality $|z_2\epsilon_2| \le (1/2)z_2^2 + (1/2)\epsilon_2^2$, we have

$$\dot{V}_2 \le -\zeta_2 z_2^2 + \rho_c z_2 + z_2 z_3 + \frac{1}{2}\epsilon_2^2 + \sigma_4 \tilde{\theta}_2^\top \hat{\theta}_2 + \sigma_5 \tilde{\psi}_2 \hat{\psi}_2 + C_2. \quad (44)$$

Remark 3: In the second step, the controllability of the nonaffine nonlinear function $\phi_3(x_2, x_3)$ is analyzed by using the mean value theorem and deriving Property 2. Then, the adaptive virtual control law (40) with adaptive laws (41) and (42) is constructed using the Lyapunov stability analysis. In the Lyapunov-based control design, the adaptive laws (41) and (42) are derived to tune the weighting vector of the neural-network-based function approximator $\hat{\theta}_2^\top \xi_2$ and to compensate for the unknown reconstruction error ψ_2, respectively.

Step 3: Consider $\dot{x}_3 = \phi_4(x_2, x_3) + bu$. A Lyapunov function candidate V_3 is chosen as

$$V_3 = \frac{1}{2}\bar{b} z_3^2 + \frac{1}{2}\left(\tilde{\theta}_3^\top \gamma_6^{-1} \tilde{\theta}_3 + \gamma_7^{-1}\tilde{\psi}_3^2 + \gamma_8^{-1}\tilde{b}^2\right) \quad (45)$$

where $\tilde{\theta}_3 = \theta_3^* - \hat{\theta}_3$, $\tilde{\psi}_3 = \psi_3^* - \hat{\psi}_3$, and $\tilde{b} = \bar{b} - \hat{b}$; $\hat{\theta}_3$, $\hat{\psi}_3$, and $\hat{b}$ are estimates of θ_3^*, ψ_3^*, and $\bar{b} = 1/b$, respectively, $\gamma_6 > 0$ is a tuning matrix, and $\gamma_7 > 0$ and $\gamma_8 > 0$ are tuning gains.

The time derivative of V_3 gives

$$\dot{V}_3 = z_3(u + W_3(\varrho_3) - \bar{b}\dot{\alpha}_{2f}) - \tilde{\theta}_3^\top \gamma_6^{-1}\dot{\hat{\theta}}_3 - \gamma_7^{-1}\tilde{\psi}_3\dot{\hat{\psi}}_3 - \gamma_8^{-1}\tilde{b}\dot{\hat{b}} \quad (46)$$

where $W_3(\varrho_3) = \bar{b}\phi_4(\varrho_3)$; $\varrho_3 = [x_2, x_3]^\top$.

By substituting $W_3 = \theta_3^{*\top}\xi_3 + \psi_3$ into (46) and using the inequality

$$z_3\psi_3 \le z_3 \tanh\left(\frac{z_3}{\kappa_3}\right)\psi_3^* + 0.2785\kappa_3\psi_3^* \quad (47)$$

with a constant $\kappa_3 > 0$, (46) becomes

$$\dot{V}_3 = z_3\left(u + \theta_3^{*\top}\xi_3 + \tanh\left(\frac{z_3}{\kappa_3}\right)\psi_3^* - \bar{b}\dot{\alpha}_{2f}\right) - \tilde{\theta}_3^\top \gamma_6^{-1}\dot{\hat{\theta}}_3 - \gamma_7^{-1}\tilde{\psi}_3\dot{\hat{\psi}}_3 - \gamma_8^{-1}\tilde{b}\dot{\hat{b}} + C_3 \quad (48)$$

where $C_3 = 0.2785\kappa_3\psi_3^*$.

Finally, we derive an adaptive actual control law u as follows:

$$u = -\zeta_3 z_3 - z_2 - \hat{\theta}_3^\top \xi_3 - \tanh\left(\frac{z_3}{\kappa_3}\right)\hat{\psi}_3 + \hat{b}\frac{\alpha_2 - \alpha_{2f}}{\nu_2} \quad (49)$$

$$\dot{\hat{\theta}}_3 = \gamma_6(z_3\xi_3 - \sigma_6\hat{\theta}_3) \quad (50)$$

$$\dot{\hat{\psi}}_3 = \gamma_7\left(\rho \tanh\left(\frac{z_3}{\kappa_3}\right) - \sigma_7\hat{\psi}_3\right) \quad (51)$$

$$\dot{\hat{b}} = \gamma_8\left(-z_3\frac{\alpha_2 - \alpha_{2f}}{\nu_2} - \sigma_8\hat{b}\right) \quad (52)$$

where $\zeta_3 > 0$ is a control gain and $\sigma_6, \sigma_7, \sigma_8 > 0$ denote the design parameters for the σ-modification [28].

Substituting (49)–(52) into (48), we get

$$\dot{V}_3 \le -\zeta_3 z_3^2 - z_2 z_3 + \sigma_6\tilde{\theta}_3^\top\hat{\theta}_3 + \sigma_7\tilde{\psi}_3\hat{\psi}_3 + \sigma_8\tilde{b}\hat{b} + C_3. \quad (53)$$

Remark 4: In the third step, the actual control law (49) with adaptive laws (50)–(52) is designed using the Lyapunov stability theorem. In the Lyapunov-based control design, the adaptive laws (41) and (42) are derived to tune the weighting vector of the neural-network-based function approximator $\hat{\theta}_3^\top\xi_3$ and to compensate for the unknown reconstruction error ψ_3, respectively. Furthermore, the adaptive law (52) is designed to compensate for the unknown parameter $\bar{b}$.

Remark 5: The previous temperature control results [11]–[17] for PEMFC thermal management systems did not consider the dynamic property of the coolant pump and the temperature constraint problem to prevent the membrane dehydration and electrode flooding. However, we consider the nonlinear dynamics of the coolant circuit (12) with the non-affine and affine nonlinearities ϕ_3 and ϕ_4 in the constrained thermal management systems (13). By deriving two physical properties (i.e., Properties 1 and 2) for the recursive control design, we construct the approximation-based adaptive temperature control scheme (i.e., (28)–(31), (40)–(42) and (49)–(52)), as shown in Fig. 1. Moreover, all system parameters and nonlinearities can be compensated by the proposed adaptive approximation control scheme, compared to [11]–[17].

C. STABILITY ANALYSIS

This section focuses on the stability analysis of the proposed control system. The dynamics of the boundary layer errors are follow as

$$\dot{\epsilon}_1 = -\frac{\epsilon_1}{\nu_1} + N_1(z_1, z_2, \epsilon_1, \hat{\theta}_1, \hat{\psi}_1, \hat{a})$$
$$\dot{\epsilon}_2 = -\frac{\epsilon_2}{\nu_2} + N_2(z_1, z_2, z_3, \epsilon_1, \epsilon_2, \hat{\theta}_1, \hat{\theta}_2, \hat{\psi}_1, \hat{\psi}_2, \hat{a}) \quad (54)$$

and

$$N_1 = -\zeta_1\dot{z}_1 - \frac{\dot{\rho}_c}{2} - \dot{\hat{\theta}}_1^\top\xi_1 - \hat{\theta}_1^\top\dot{\xi}_1 - \operatorname{sech}^2\left(\frac{\rho_c}{\kappa_1}\right)\frac{\dot{\rho}_c}{\kappa_1}\hat{\psi}_1 - \tanh\left(\frac{\rho_c}{\kappa_1}\right)\dot{\hat{\psi}}_1 - \operatorname{sech}^2\left(\frac{\rho_c}{\kappa_0}\right)\frac{\dot{\rho}_c}{\kappa_0}\hat{a}\delta - \tanh\left(\frac{\rho_c}{\kappa_0}\right)\dot{\hat{a}}\delta - \tanh\left(\frac{\rho_c}{\kappa_0}\right)\hat{a}\dot{\delta}$$

$$N_2 = \zeta_2\dot{z}_2 - \dot{\rho}_c + \dot{\hat{\theta}}_2^\top\xi_2 + \hat{\theta}_2^\top\dot{\xi}_2 + \tanh\left(\frac{z_2}{\kappa_2}\right)\dot{\hat{\psi}}_2 + \operatorname{sech}^2\left(\frac{z_2}{\kappa_2}\right)\frac{\dot{z}_2}{\kappa_2}\hat{\psi}_2 + \frac{1}{2}\dot{z}_2.$$

Consider the following total Lyapunov function V

$$V = V_1 + V_2 + V_3 + \frac{1}{2}\epsilon_1^2 + \frac{1}{2}\epsilon_2^2. \quad (55)$$

Remark 6: The total Lyapunov function V in (55) consists of the Lyapunov functions V_1, V_2, and V_3 used in the design steps and the boundary layer errors ϵ_1 and ϵ_2 for the first-order filtering of the virtual control laws. The function V is

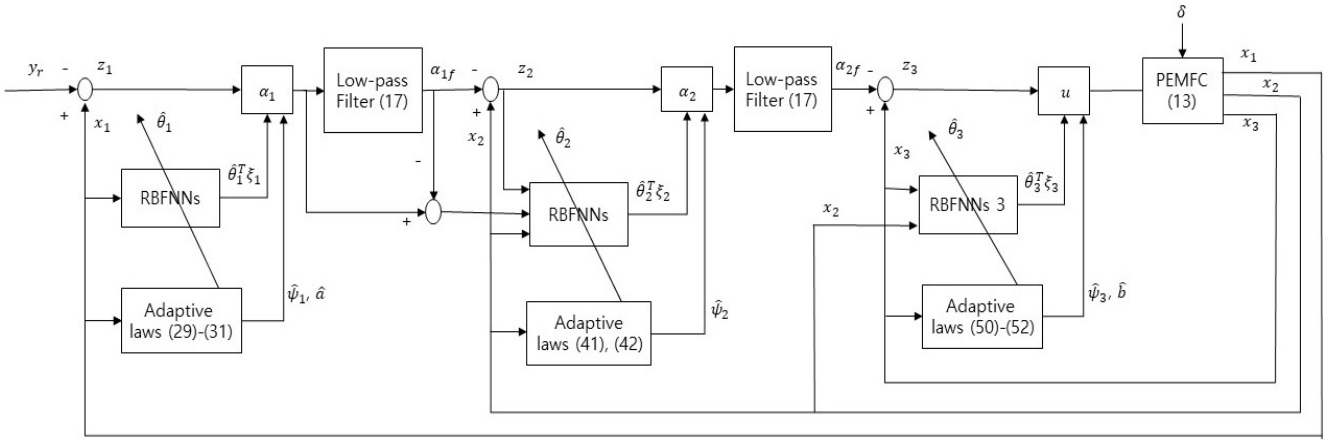

FIGURE 1. Block Diagram of the proposed adaptive control system.

defined to analyze the stability of the controlled closed-loop system. The inequalities (33), (44), and (53) induced from the control design steps are used for the stability analysis in the proof of the following theorem.

Theorem 1: Consider the uncertain nonlinear thermal management system (13) with the temperature constraint (14). For any initial conditions satisfying $V(0) \leq l$ with a constant $l > 0$ and $y_r - k_c < y(0) < y_r + k_c$, the proposed adaptive control scheme consisting of (28)–(31), (40)–(42) and (49)–(52) ensures that all the signals in the closed-loop system are uniformly ultimately bounded and the control error converges to a neighborhood of the origin while the stack temperature remains within constraints.

Proof: From (33), (44), (53), and (54), the time derivative of V becomes

$$\begin{aligned}\dot{V} \leq & -\zeta_1\rho_c z_1 - \zeta_2 z_2^2 - \zeta_3 z_3^2 - \frac{1}{\nu_1}\epsilon_1^2 + \frac{1}{2}\epsilon_1^2 + \epsilon_1 N_1 \\ & -\frac{1}{\nu_2}\epsilon_2^2 + \frac{1}{2}\epsilon_2^2 + \epsilon_2 N_2 - \frac{\sigma_1}{2}\|\tilde{\theta}_1\|^2 - \frac{\sigma_2}{2}\tilde{\psi}_1^2 - \frac{\sigma_3}{2}\tilde{a}^2 \\ & -\frac{\sigma_4}{2}\|\tilde{\theta}_2\|^2 - \frac{\sigma_5}{2}\tilde{\psi}_2^2 - \frac{\sigma_6}{2}\|\tilde{\theta}_3\|^2 - \frac{\sigma_7}{2}\tilde{\psi}_3^2 \\ & -\frac{\sigma_8}{2}\tilde{b}^2 + \frac{\sigma_1}{2}\bar{\theta}_1^2 + \frac{\sigma_2}{2}(\psi_1^*)^2 + \frac{\sigma_3}{2}\bar{a}^2 + \frac{\sigma_4}{2}\bar{\theta}_2^2 \\ & +\frac{\sigma_5}{2}(\psi_2^*)^2 + \frac{\sigma_6}{2}\bar{\theta}_3^2 + \frac{\sigma_7}{2}(\psi_3^*)^2 + \frac{\sigma_8}{2}\bar{b}^2 \\ & +C_1 + C_2 + C_3. \end{aligned} \tag{56}$$

Consider the set $\Pi := \{(1/\phi_2)\log(k_c^2/(k_c^2 - z_1^2)) + z_2^2 + z_3^2 + \tilde{\theta}_1^\top\gamma_1^{-1}\tilde{\theta}_1 + \gamma_2^{-1}\tilde{\psi}_1^2 + \gamma_3^{-1}\tilde{a}^2 + \tilde{\theta}_2^\top\gamma_4^{-1}\tilde{\theta}_2 + \gamma_5^{-1}\tilde{\psi}_2^2 + \tilde{\theta}_3^\top\gamma_6^{-1}\tilde{\theta}_3 + \gamma_7^{-1}\tilde{\psi}_3^2 + \gamma_8^{-1}\tilde{b}^2 + \epsilon_1^2 + \epsilon_2^2 \leq 2l\}$. Since Π is compact in $\mathbb{R}^{10+r_1+r_2+r_3}$, $|N| \leq B$ is satisfied on Π where $B > 0$ is a constant. From the inequality $\epsilon_i N_i \leq N_i^2\epsilon_i^2/2 + 1/2$, $i = 1, 2$, (56) becomes

$$\begin{aligned}\dot{V} \leq & -\zeta_1\rho z_1 - \zeta_2 z_2^2 - \zeta_3 z_3^2 - \sum_{i=1}^{2}\left(\frac{1}{\nu_i} - \frac{1}{2} - \frac{N_i^2}{2}\right)\epsilon_i^2 \\ & -\frac{\sigma_1}{2}\|\tilde{\theta}_1\|^2 - \frac{\sigma_2}{2}\tilde{\psi}_1^2 - \frac{\sigma_3}{2}\tilde{a}^2 - \frac{\sigma_4}{2}\|\tilde{\theta}_2\|^2 - \frac{\sigma_5}{2}\tilde{\psi}_2^2 \\ & -\frac{\sigma_6}{2}\|\tilde{\theta}_3\|^2 - \frac{\sigma_7}{2}\tilde{\psi}_3^2 - \frac{\sigma_8}{2}\tilde{b}^2 + C \end{aligned} \tag{57}$$

where $C = C_1 + C_2 + C_3 + 1 + (1/2)[\bar{\theta}_1^2 + (\psi_1^*)^2 + \bar{a}^2 + \bar{\theta}_2^2 + (\psi_2^*)^2 + \bar{\theta}_3^2 + (\psi_3^*)^2 + \bar{b}^2]$.

From Lemma 2, we have $-\zeta_1\rho_c z_1 \leq -\zeta_1 z_1^2$. Then, choosing $1/\nu_i = 1/2 + B_i^2/2 + \bar{\nu}_i$ with a constant $\bar{\nu}_i > 0$ and $i = 1, 2$, we obtain

$$\begin{aligned}\dot{V} \leq & -\zeta_1 z_1^2 - \zeta_2 z_2^2 - \zeta_3 z_3^2 - \sum_{i=1}^{2}\bar{\nu}_i\epsilon_i^2 - \frac{\sigma_1}{2}\|\tilde{\theta}_1\|^2 \\ & -\frac{\sigma_2}{2}\tilde{\psi}_1^2 - \frac{\sigma_3}{2}\tilde{a}^2 - \frac{\sigma_4}{2}\|\tilde{\theta}_2\|^2 - \frac{\sigma_5}{2}\tilde{\psi}_2^2 - \frac{\sigma_6}{2}\|\tilde{\theta}_3\|^2 \\ & -\frac{\sigma_7}{2}\tilde{\psi}_3^2 - \frac{\sigma_8}{2}\tilde{b}^2 - \sum_{i=1}^{2}\left(1 - \frac{N_i^2}{B_i^2}\right)\frac{B_i^2\epsilon_i^2}{2} + C. \end{aligned} \tag{58}$$

Then, $\dot{V} \leq -KV + C$ is satisfied on $V = l$ where $K = \min\{2\zeta_1\phi_2, 2\zeta_2, 2\zeta_3, 2\bar{\nu}_i, \sigma_1/(\lambda_{\max}(\gamma_1^{-1})), \sigma_2\gamma_2, \sigma_3\gamma_3, \sigma_4/(\lambda_{\max}(\gamma_4^{-1})), \sigma_5\gamma_5, \sigma_6/(\lambda_{\max}(\gamma_6^{-1})), \sigma_7\gamma_7, \sigma_8\gamma_8\}$. When $K > C/l$, $\dot{V} < 0$ that leads to the uniform ultimate boundedness of all closed-loop signals. Since V_{z_1} is bounded, the stack temperature constraint $-k_c < z_1(t) < k_c$ is satisfied for all $t \geq 0$. The boundedness of x_1 yields $|\phi_2| \leq \bar{\phi}_2$. From $\dot{V} \leq -KV + C$, we have $V_{z_1}/\bar{\phi}_2 \leq V(t) \leq e^{-Kt}V(0) + (C/K)(1 - e^{-Kt})$. Then, we have $|\varphi_c| \leq \sqrt{1 - e^{-2\bar{\phi}_2[V(0)e^{-Kt} + (C/K)(1-e^{-Kt})]}}$. As $t \to \infty$, $|\varphi_c| \leq \sqrt{1 - e^{-(2\bar{\phi}_2(C/K))}}$. Thus, the control error z_1 can be reduced by adjusting design parameters. ■

Remark 7: Based on the proof of Theorem 1, some guidelines for the choice of the design parameters are given as follows.

1) As ζ_1, ζ_2, and ζ_3 increase, K increases. Thus, the bound $\sqrt{1 - e^{-2\bar{\phi}_2(C/K)}}$ of φ_c can be reduced, namely, the control error z_1 is reduced.

2) As κ_i decreases, C is reduced. Subsequently, the bound $\sqrt{1 - e^{-2\bar{\phi}_2(C/K)}}$ of φ_c can be reduced, namely, the control error z_1 is reduced.

3) The adaptive parameters $\hat{\theta}_i$, $\hat{\psi}_i$, $\hat{a}$, and $\hat{b}$, $i = 1, 2, 3$, can be tuned rapidly by increasing γ_i and fixing σ_i as small constants.

V. SIMULATION RESULTS

Consider the nonlinear thermal management system (13) with the nonlinear coolant circuit dynamics. Different from

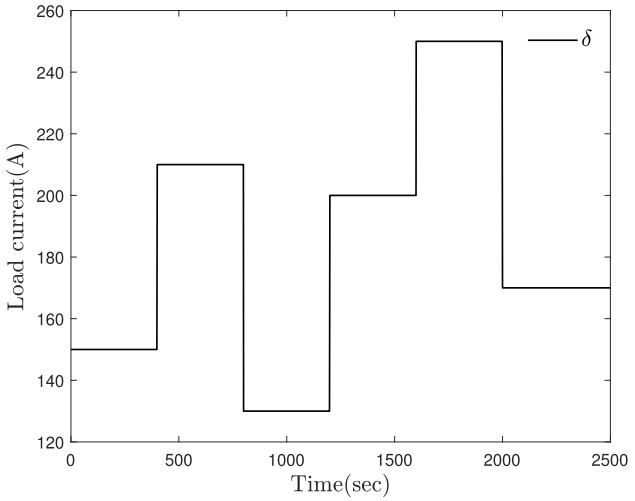

FIGURE 2. Load current.

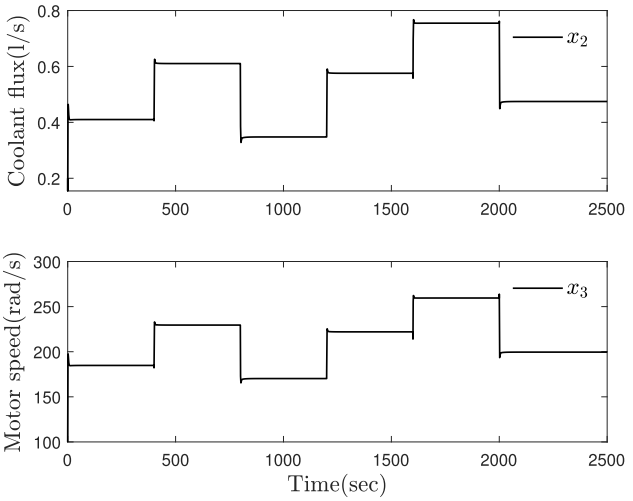

FIGURE 4. Coolant flux x_2 and motor speed x_3 of the proposed control system.

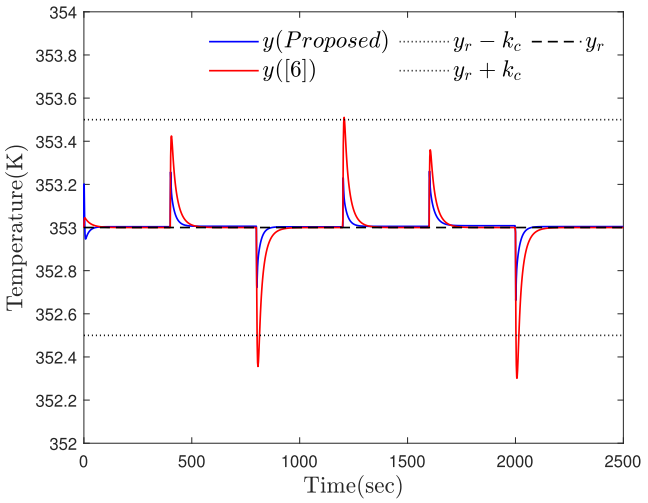

FIGURE 3. Comparison of temperature control results.

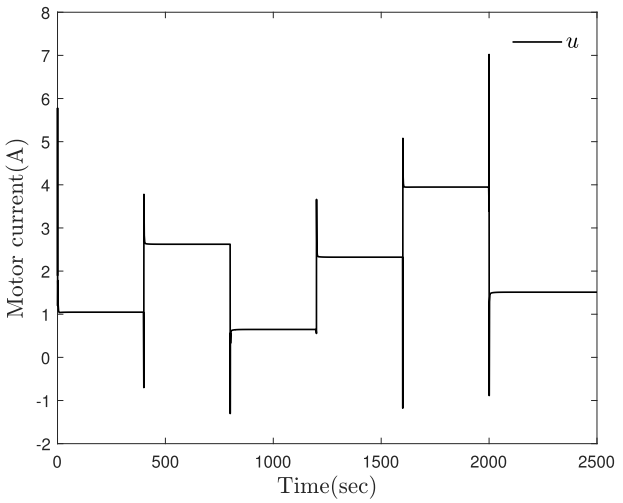

FIGURE 5. Control input of the proposed control system.

the existing temperature control methods [5]–[8], [11]–[17], the proposed adaptive thermal controller firstly deals with the nonlinear coolant circuit dynamics of PEMFCs. Thus, the controller [6] considering only the thermal management model (10) is used for the simulation comparison about the temperature constraint satisfaction. The load current δ is shown in Fig. 2 and the initial values of the state variables are $x_1(0) = 353$, $x_2(0) = 0.2$, and $x_3(0) = 100$. For the temperature constraint, we choose $k_c = 0.5$. The design parameters for the proposed controller are adopted as $\zeta_1 = 1$, $\zeta_2 = 400$, $\zeta_3 = 0.1$, $\nu_1 = \nu_2 = 0.01$, $\kappa_i = 5$, $\gamma_1 = \text{diag}[0.5]$, $\gamma_2 = 10$, $\gamma_3 = 1$, $\gamma_4 = \text{diag}[50]$, $\gamma_5 = 1$, $\gamma_6 = \text{diag}[0.01]$, $\gamma_7 = 0.1$, $\gamma_8 = 10^{-7}$, $\sigma_j = 10^{-3}$, $\sigma_3 = 0.005$, $\sigma_5 = 0.1$, $\sigma_7 = 0.1$, and $\sigma_8 = 10^3$ where $i = 0, \ldots, 3$ and $j = 1, 2, 4, 6$.

The adaptive regulation results of the stack temperature to $y_r = 353$ are compared in Fig. 3. While the temperature response using the controller [6] violates the temperature constraint according to the change of the load current, the output response of the proposed adaptive thermal control system is ensured within stack temperature constraints. The coolant flux and motor speed of coolant circuit of the proposed adaptive control system are depicted in Fig. 4. The pump motor current for the control input of the proposed control system is displayed in Fig. 5. Fig. 6 shows the outputs of the RBFNNs and the parameter estimates used in the proposed control system. In these figures, we can see that the proposed adaptive control has good regulation performance while the stack temperature remains within constraints for preventing the membrane dehydration and electrode flooding of nonlinear PEMFCs. Furthermore, the control result reveals that the dynamic load current and the parametric and non-parametric uncertainties can be overcome by establishing the approximation-based adaptive control strategy although the uncertain nonlinear coolant circuit dynamics is considered in the thermal management systems.

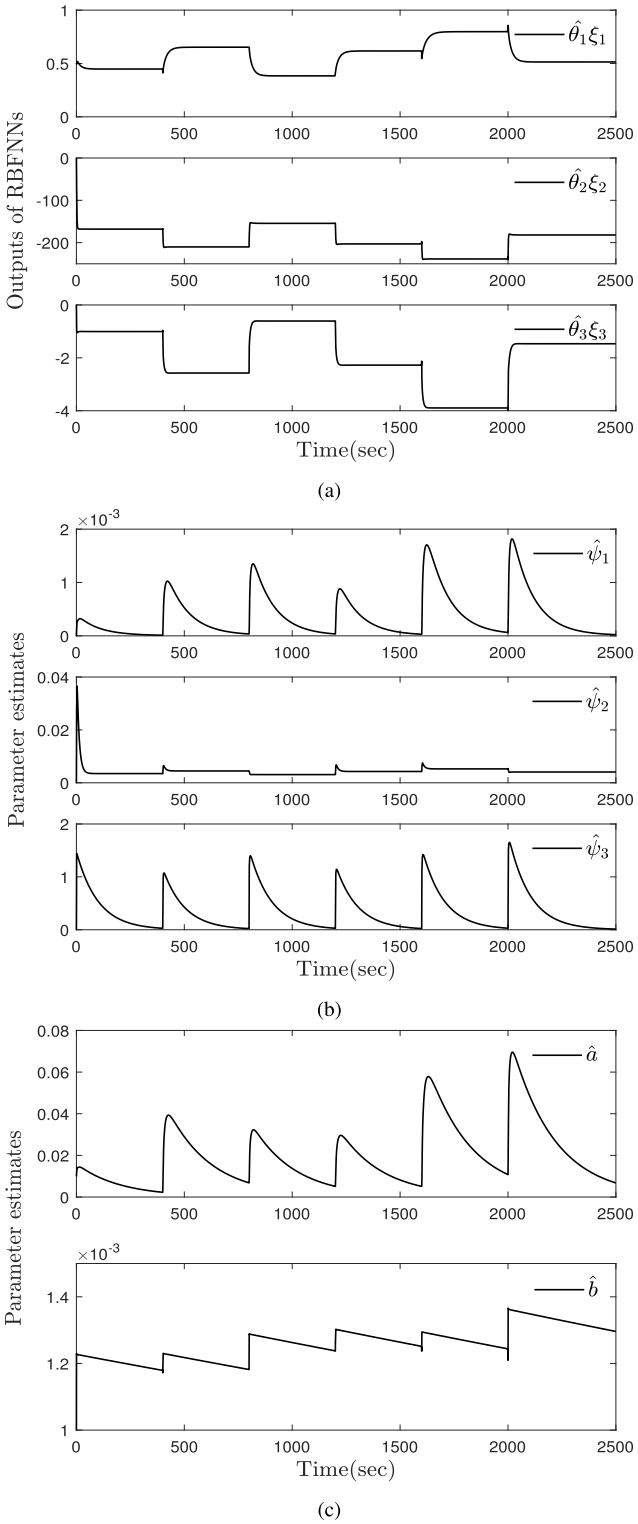

FIGURE 6. RBFNN outputs and adaptive parameters of the proposed control system (a) $\hat{\theta}_1^\top\xi_1$, $\hat{\theta}_2^\top\xi_2$, and $\hat{\theta}_3^\top\xi_3$ (b) $\hat{\psi}_1$,$\hat{\psi}_2$, and $\hat{\psi}_3$ (c) $\hat{a}$ and $\hat{b}$.

VI. CONCLUSION

The paper has established the adaptive temperature control strategy for avoiding the membrane dehydration and electrode flooding of uncertain thermal management systems with nonlinear coolant circuit dynamics of nonlinear PEMFCs. The coolant circuit model including the nonlinear coolant flux and pump dynamics has been firstly combined with the nonlinear stack temperature dynamics in temperature control field. Then, an adaptive temperature control scheme has been constructed to guarantee the robust temperature regulation within the stack temperature constraints even though all system parameters and nonlinearities are unknown and the external load changes suddenly. A Lyapunov-based analysis method has been derived to prove the convergence of the control error while all closed-loop signals remain bounded.

REFERENCES

[1] W. R. W. Daud, R. E. Rosli, E. H. Majlan, S. A. A. Hamid, R. Mohamed, and T. Husaini, "PEM fuel cell system control: A review," *Renew. Energy*, vol. 113, pp. 620–638, Dec. 2017.

[2] O. Z. Sharaf and M. F. Orhan, "An overview of fuel cell technology: Fundamentals and applications," *Renew. Sustain. Energy Rev.*, vol. 32, pp. 810–853, Apr. 2014.

[3] J. T. Pukrushpan, A. G. Stefanopoulou, and H. Peng, *Control of Fuel Cell Power Systems: Principles, Modeling, Analysis and Feedback Design* London, U.K.: Springer-Verlag, 2004.

[4] X. Li, Z.-H. Deng, D. Wei, C.-S. Xu, and G.-Y. Cao, "Novel variable structure control for the temperature of PEM fuel cell stack based on the dynamic thermal affine model," *Energy Convers. Manage.*, vol. 52, no. 11, pp. 3265–3274, Oct. 2011.

[5] L. A. M. Riascos and D. D. Pereira, "Optimal temperature control in PEM fuel cells," in *Proc. 35th Annu. Conf. IEEE Ind. Electron.*, Nov. 2009, pp. 2778–2783.

[6] D. Li, C. Li, Z. Gao, and Q. Jin, "On active disturbance rejection in temperature regulation of the proton exchange membrane fuel cells," *J. Power Sources*, vol. 283, pp. 452–463, Jun. 2015.

[7] L. Huang, J. Chen, Z. Liu, and M. Becherif, "Adaptive thermal control for PEMFC systems with guaranteed performance," *Int. J. Hydrogen Energy*, vol. 43, no. 25, pp. 11550–11558, Jun. 2018.

[8] C. Yan, J. Chen, H. Liu, and H. Lu, "Model-based fault tolerant control for the thermal management of PEMFC systems," *IEEE Trans. Ind. Electron.*, vol. 67, no. 4, pp. 2875–2884, Apr. 2020.

[9] S. G. Kandlikar and Z. Lu, "Thermal management issues in a PEMFC stack—A brief review of current status," *Appl. Thermal Eng.*, vol. 29, no. 7, pp. 1276–1280, May 2009.

[10] X. Yu, B. Zhou, and A. Sobiesiak, "Water and thermal management for ballard PEM fuel cell stack," *J. Power Sources*, vol. 147, nos. 1–2, pp. 184–195, Sep. 2005.

[11] J.-W. Ahn and S.-Y. Choe, "Coolant controls of a PEM fuel cell system," *J. Power Sources*, vol. 179, no. 1, pp. 252–264, Apr. 2008.

[12] X. Zhao, Y. Li, Z. Liu, Q. Li, and W. Chen, "Thermal management system modeling of a water-cooled proton exchange membrane fuel cell," *Int. J. Hydrogen Energy*, vol. 40, no. 7, pp. 3048–3056, Feb. 2015.

[13] J. Han, J. Park, and S. Yu, "Control strategy of cooling system for the optimization of parasitic power of automotive fuel cell system," *Int. J. Hydrogen Energy*, vol. 40, no. 39, pp. 13549–13557, Oct. 2015.

[14] J. Han, S. Yu, and S. Yi, "Advanced thermal management of automotive fuel cells using a model reference adaptive control algorithm," *Int. J. Hydrogen Energy*, vol. 42, no. 7, pp. 4328–4341, Feb. 2017.

[15] J. D. Rojas, C. Ocampo-Martinez, and C. Kunusch, "Thermal modelling approach and model predictive control of a water-cooled PEM fuel cell system," in *Proc. IECON 39th Annu. Conf. IEEE Ind. Electron. Soc.*, Nov. 2013, pp. 3806–3811.

[16] P. Hu, G.-Y. Cao, X.-J. Zhu, and M. Hu, "Coolant circuit modeling and temperature fuzzy control of proton exchange membrane fuel cells," *Int. J. Hydrogen Energy*, vol. 35, no. 17, pp. 9110–9123, Sep. 2010.

[17] C. Fang, L. Xu, S. Cheng, J. Li, H. Jiang, and M. Ouyang, "Sliding-mode-based temperature regulation of a proton exchange membrane fuel cell test bench," *Int. J. Hydrogen Energy*, vol. 42, no. 16, pp. 11745–11757, Apr. 2017.

[18] G. Vasu and A. K. Tangirala, "Control-orientated thermal model for proton-exchange membrane fuel cell systems," *J. Power Sources*, vol. 183, no. 1, pp. 98–108, Aug. 2008.

[19] K. P. Tee, S. S. Ge, and E. H. Tay, "Barrier Lyapunov functions for the control of output-constrained nonlinear systems," *Automatica*, vol. 45, no. 4, pp. 918–927, Apr. 2009.
[20] D. Swaroop, J. K. Hedrick, P. P. Yip, and J. C. Gerdes, "Dynamic surface control for a class of nonlinear systems," *IEEE Trans. Autom. Control*, vol. 45, no. 10, pp. 1893–1899, Oct. 2000.
[21] J. T. Pukrushpan, H. Peng, and A. G. Stefanopoulou, "Control-oriented modeling and analysis for automotive fuel cell systems," *J. Dyn. Syst., Meas., Control*, vol. 126, no. 1, pp. 14–25, Mar. 2004.
[22] J. C. Amphlett, R. M. Baumert, R. F. Mann, B. A. Peppley, P. R. Roberge, and T. J. Harris, "Performance modeling of the ballard mark IV solid polymer electrolyte fuel cell," *J. Electrochem. Soc.*, vol. 142, no. 1, p. 9, 1995.
[23] M. M. Polycarpou, "Stable adaptive neural control scheme for nonlinear systems," *IEEE Trans. Autom. Control*, vol. 41, no. 3, pp. 447–451, Mar. 1996.
[24] Z. Zhao, W. He, and S. Sam Ge, "Adaptive neural network control of a fully actuated marine surface vessel with multiple output constraints," *IEEE Trans. Control Syst. Technol.*, vol. 22, no. 4, pp. 1536–1543, Jul. 2014.
[25] C. Wang, D. J. Hill, S. S. Ge, and G. Chen, "An ISS-modular approach for adaptive neural control of pure-feedback systems," *Automatica*, vol. 42, no. 5, pp. 723–731, May 2006.
[26] A. J. Kurdila, F. J. Narcowich, and J. D. Ward, "Persistency of excitation in identification using radial basis function approximants," *SIAM J. Control Optim.*, vol. 33, no. 2, pp. 625–642, Mar. 1995.
[27] H. K. Khalil, *Nonlinear Systems*. Upper Saddle River, NJ, USA: Prentice-Hall, 1996.
[28] P. A. Ioannou and P. V. Kokotovic, *Adaptive Systems with Reduced Models*. New York, NY, USA: Springer-Verlag, 1983.
[29] H. Jeffreys, *Methods of Mathematical Physics*. Cambridge, U.K.: Cambridge Univ. Press, 1988.

BYUNG MO KIM received the B.S. degree from the School of Electrical and Electronics Engineering, Chung-Ang University, Seoul, South Korea, in 2019, where he is currently pursuing the master's degree with the Department of Electrical and Electronic Engineering. His current research interests include nonlinear adaptive control and intelligent control using neural networks.

SUNG JIN YOO received the B.S., M.S., and Ph.D. degrees in electrical and electronic engineering from Yonsei University, Seoul, South Korea, in 2003, 2005, and 2009 respectively. He was a Postdoctoral Researcher with the Department of Mechanical Science and Engineering, University of Illinois at Urbana–Champaign, Illinois, from 2009 to 2010. Since 2011, he has been with the School of Electrical and Electronics Engineering, Chung-Ang University, Seoul, where he is currently a Professor. His research interests include nonlinear adaptive control, decentralized control, distributed control, fault-tolerant control, and neural networks theories and their applications to robotic, flight, nonlinear time-delay systems, large-scale systems, and multiagent systems.